

PROTON EMITTERS: A LABORATORY FOR  
DETAILED NUCLEAR STRUCTURE STUDIES  
BEYOND THE DRIP LINE\* \*\*

D. SEWERYNIAK, C.N. DAVIDS, A. HEINZ, G. MUKHERJEE

Argonne National Laboratory, Argonne, IL 60439, USA

P.J. WOODS, T. DAVINSON, H. MAHMUD, P. MUNRO, A. ROBINSON

University of Edinburgh, Edinburgh, United Kingdom

J.J. RESSLER, J. SHERGUR, W.B. WALTERS, AND A. WÖHR

University of Maryland, College Park, Maryland 20742, USA

*(Received January 9, 2003)*

The structure of nuclei situated far from the line of  $\beta$  stability is presently one of the major thrusts in nuclear physics. The phenomenon of proton emission offers a unique opportunity to study nuclei beyond the proton dripline. Within the last decade proton-decay studies have been transformed from a curiosity into a powerful spectroscopic tool. Experimental effort has resulted in the observation of deformed proton emitters, the discovery of proton-decay fine structure and the observation of excited states in several proton emitters. Thank to continuous progress in experimental techniques the body of data on proton emission is steadily increasing. Several theoretical models have been developed to quantitatively reproduce proton-decay widths. The role of Coriolis mixing, non-axial degrees of freedom, proton-neutron interaction, coupling to core vibrations are some of the aspects currently under investigation. This paper discusses recent progress on the understanding of proton decay. It will be illustrated by experimental results obtained at the Argonne National Laboratory within the last 2 years.

PACS numbers: 23.50.+z

---

\* Presented at the XXXVII Zakopane School of Physics "Trends in Nuclear Physics", Zakopane, Poland, September 3–10, 2002.

\*\* Supported by the U.S. Department of Energy, Nuclear Physics Division, under contract No. W-31-109-ENG-38.

## 1. Introduction

Spontaneous proton emission takes place in proton rich nuclei having a negative proton separation energy. Protons are held inside the nucleus by the Coulomb and the centrifugal barrier and the decay proceeds via quantum tunneling. Proton decay is analogous to  $\alpha$  decay. However, there is no pre-formation factor involved which simplifies the process. In addition, the centrifugal barrier is relatively more important for proton decay. As a result, proton-decay widths are very sensitive to the angular momentum of the states involved in the decay, and thus to their structure.

Proton emitters are a laboratory to study quantum tunneling through a 3-dimensional barrier. They provide information on single-particle energies,  $j$ -content of the wave functions, shape of the mean-field potential, and proton separation energies far from the line of stability.

The first proton emitting isomer  $^{53m}\text{Co}$  was discovered in 1970 at Harwell [1]. The first ground-state proton emitter  $^{151}\text{Lu}$  was discovered at GSI in 1974 using the velocity filter SHIP [2]. The introduction of recoil mass separators coupled with Double-Sided Si detectors brought a renaissance in proton-decay studies in the late 1990s. Presently, 28 proton emitters are known with atomic numbers between 51 and 81. Most of the proton emitters are spherical. Anomalous decay rates in  $^{131}\text{Eu}$  and  $^{141}\text{Ho}$  were explained by large deformation [3]. The first case of the proton fine structure was found in  $^{131}\text{Eu}$  [4]. A weak branch to the  $2^+$  excited state in the daughter nucleus was proposed. The Recoil-Decay Tagging method [5] allowed to observe excited states in several proton emitters. For example, rotational bands were identified in  $^{141}\text{Ho}$  [6]. Proton emission from excited rotational bands was also reported in several nuclei in the vicinity of  $^{56}\text{Ni}$  [7]. Recently, the first 2-proton emitter  $^{45}\text{Fe}$  was observed independently as a product of projectile fragmentation reactions at GANIL [8] and GSI [9].

## 2. Models of proton decay

There exist several theoretical models describing proton decay both for spherical and deformed nuclei [3, 10–13]. In one approach the Schrödinger equation is solved inside the nucleus using the Woods–Saxon mean-field potential with the depth adjusted to reproduce the measured proton-decay  $Q$ -value. Subsequently, the resulting wave function is matched outside the nucleus with an outgoing Coulomb wave. The proton-decay width is obtained by integrating the outgoing particle flux. In order to account for pairing the so called spectroscopic factor is introduced reflecting the probability that the proton orbital, which participates in the decay, is empty in the daughter nucleus.

In the case of a ground-state to ground-state proton decay in odd- $Z$ , even- $N$  spherical nuclei the proton occupying a state with angular momentum  $j_p$  simply falls off the core (see Fig. 1(a)). This approach treats the initial state as a pure single-particle state. In transitional nuclei, mixing with the low lying vibrational excitations, especially the  $2^+$  state, should be considered. It opens a decay channel to the  $2^+$  vibrational state in the daughter nucleus. The coupling to the  $2^+$  state allows proton single-particle states with lower  $j_p$  to contribute to the decay which compensates for the lower decay energy. A model for calculating branching ratios to  $2^+$  vibrational states was proposed recently in Ref. [14].

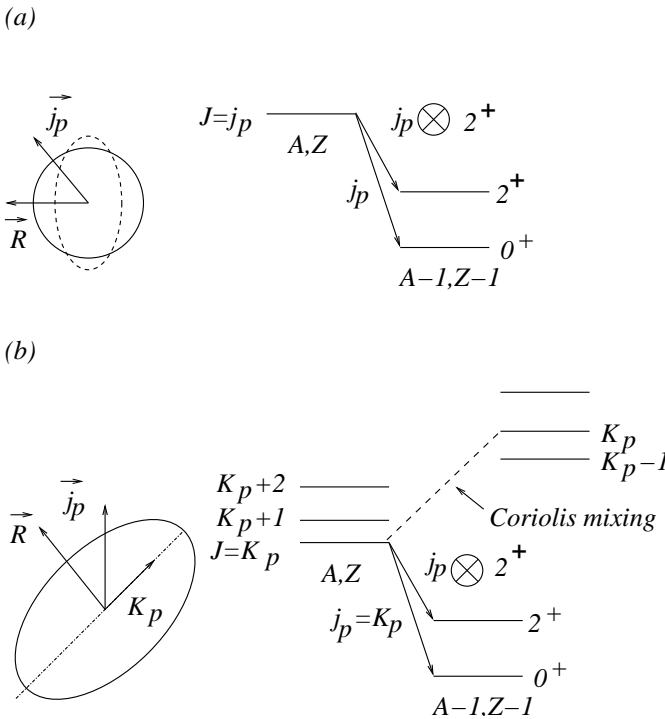


Fig. 1. Schematic view of proton decay from a (a) spherical and (b) deformed state with angular momentum  $J = j_p$  and  $J = K_p$ , respectively, in the  ${}^A_Z X$  nucleus.  $\vec{R}$  stands for the angular momentum of the core due to (a) vibration and (b) rotation.

In deformed nuclei the wave function of the decaying state is a mixture of several spherical  $j_p$  components. In the strong coupling limit only the angular momentum projection on the symmetry axis,  $K = K_p$ , is a good quantum number. The decay proceeds from the bottom of a rotational band with spin  $I = K_p$  to the  $0^+$  ground state of the daughter nucleus (see Fig. 1(b)). Only the spherical single-particle component with the lowest angular momentum

contributes to the decay. It is usually a small component. The decay width is proportional to the square of the amplitude  $c_{j_p l_p}$  of this component in the initial wave function. It turns out that under certain circumstances the decay to the  $2^+$  member of the rotational band can compete with the decay to the ground state despite the lower decay energy [4,11]. In this case angular momentum conservation is fulfilled by another, much larger, component of the wave function. It is worth mentioning that the Coriolis interaction mixes states with different  $K$  values. Coriolis effects are expected to play an important role at moderate deformations for high- $K$ , low  $j_p$  Nilsson orbitals.

In odd-odd nuclei the residual interaction between the odd proton and the odd neutron has to be taken into account. Because of this coupling different proton single-particle components can contribute to the decay. Contribution from different neutron states would lead to different neutron states. This would manifest itself in the proton-decay fine structure. The proton-decay rates in odd-odd deformed nuclei were calculated in Ref. [15].

The models developed so far assume axially symmetric states. The importance of more complex shapes has not been explored yet. For example, triaxiality would introduce  $\Delta K = 2$  mixing adding yet other single-particle components into the wavefunction.

### 3. Recent experimental results from the Argonne National Laboratory

Proton-decay studies require an efficient and very selective detection method. The experimental method and the setup used at the Argonne National Laboratory is shown in Fig. 2. Proton emitters are produced using heavy-ion fusion-evaporation reactions. Reaction products are separated from beam particles and dispersed according to their mass-to-charge-state ratio in the Fragment Mass Analyzer (FMA). After passing through a focal plane detector, where  $M/Q$  is measured, the recoiling nuclei are implanted into a Double-Sided Si Strip Detector (DSSD) where they subsequently decay. The DSSD is divided into many pixels and both the implantation and the decay take place in the same pixel. By using spatial and time information decay particles and implants are correlated with each other. As a result, mass number can be assigned to the observed decays and the decay time can be extracted. In addition, the energy of the emitted protons is measured in the DSSD. The proton-decay studies at ANL have been focused on completing experimental information on the proton drip-line in the rare earth region and in the vicinity of the  $Z = 82$  shell closure. Several new proton emitters were observed during the last 2 years. Individual cases are discussed in the following paragraphs.

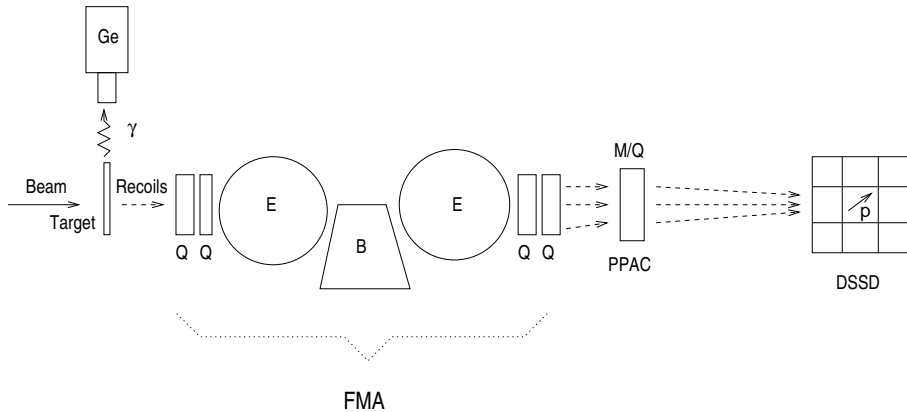


Fig. 2. The experimental setup used at ATLAS for studies of decay properties and excited states in proton emitters.

### 3.1. The $^{117}\text{La}$ nucleus

The  $^{117}\text{La}$  nucleus is expected to be situated at the onset of large quadrupole deformation. A quadrupole deformation of  $\beta_2 = 0.29$  was calculated for the  $^{117}\text{La}$  ground state [16]. Protons emitted from the  $^{117}\text{La}$  ground state have been observed for the first time at Laboratori Nazionali di Legnaro [17]. A second weak proton line has also been reported and assigned to an isomer in  $^{117}\text{La}$ . In an experiment at ANL the ground state  $^{117}\text{La}$  proton decay was confirmed [18]. More precise values for the proton energy and half life were obtained. The measured and calculated decay widths agreed with each other for the  $3/2^+ [422]g_{7/2}$  and  $3/2^- [541]h_{11/2}$  proton Nilsson orbitals. However, despite more statistics, no evidence for the isomeric proton decay was found. A search for  $^{116}\text{La}$  proton decay did not give a positive result.

### 3.2. The $^{135}\text{Tb}$ nucleus

In the quest to complete experimental information on the proton drip-line in the rare earth region an experiment was carried out to look for proton emitting Tb isotopes. The  $^{135}\text{Tb}$  nucleus is situated between the two highly deformed proton emitters  $^{131}\text{Eu}$  and  $^{141}\text{Ho}$  [3]. Möller and Nix predicted  $\beta_2 = 0.33$  for the  $^{135}\text{Tb}$  ground state [16]. The  $^{50}\text{Cr} + ^{92}\text{Mo}$  reaction was used to produce  $^{135}\text{Tb}$  after evaporating 1 proton and 6 neutrons. The measured proton spectrum associated with  $^{135}\text{Tb}$  is shown in Fig. 3. Three counts can also be seen around 120 keV below the proton line possibly due to the decay to the  $2^+$  excited state in  $^{134}\text{Gd}$  in analogy with the  $^{131}\text{Eu}$  proton decay fine structure [4]. According to calculations the  $5/2^+ [413]d_{5/2}$

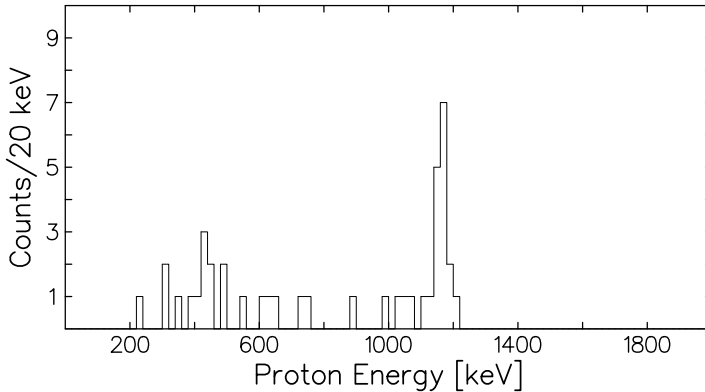


Fig. 3. The proton decay spectrum collected within 3.5 ms of implanting a mass-135 residue detected using the  $^{50}\text{Cr}+^{92}\text{Mo}$  reaction.

Nilsson orbital is the closest to the Fermi surface in  $^{135}\text{Tb}$ . Comparison of the measured half life with the proton-decay rate calculations will verify the ground-state configuration. The data analysis is in progress. The cross section estimated from the proton yield is about 2 nb. It is the first time that such a weakly produced proton emitter was observed.

### 3.3. The $^{130}\text{Eu}$ nucleus

In order to learn about the influence of an odd neutron on proton decay from deformed nuclei we studied the decay properties of  $^{130}\text{Eu}$ . The  $^{130}\text{Eu}$  odd-odd nucleus is predicted to have a quadrupole deformation of  $\beta_2=0.33$  [16]. The  $^{58}\text{Ni}(^{78}\text{Kr}, p5n)$  reaction was used to populate  $^{130}\text{Eu}$ . The data analysis revealed a group of 5 counts detected within 3 ms of the implantation of mass-130 residues. Preliminary results were published in Ref. [19]. In order to interpret the measured decay width the model presented in Ref. [15] was used to calculate decay widths from different Nilsson neutron-proton configurations. The  $3/2^+[411]d_{5/2}$  Nilsson configuration, which constitutes the ground state in  $^{131}\text{Eu}$ , was chosen for the odd proton. The  $7/2^- [523]h_{11/2}$  and  $1/2^+[411]s_{1/2}$  Nilsson states, corresponding to the ground state and the isomeric state in  $^{141}\text{Ho}$  were selected for the odd neutron. The proton number in  $^{141}\text{Ho}$  is equal to the neutron number in  $^{130}\text{Eu}$ . Both parallel and anti-parallel proton-neutron spin couplings were used in the calculations. The best agreement was obtained for the  $(K_\pi = 3/2^+ \otimes K_\nu = 1/2^+)K_T = 2^+$  configuration.

### 3.4. The $^{170}\text{Au}$ and $^{164}\text{Ir}$ nuclei

The proton emitters between Tm ( $Z = 69$ ) and Tl ( $Z = 81$ ) are spherical due to close proximity of the  $N = 82$  and  $Z = 82$  closed shells. Protons are distributed in these nuclei among three close lying orbitals, namely:  $s_{1/2}$ ,  $d_{3/2}$  and  $h_{11/2}$ . A search for two spherical odd-odd proton emitters  $^{170}\text{Au}$  and  $^{164}\text{Ir}$  was performed. Proton lines associated with both nuclei were found [19]. The  $^{164}\text{Ir}$  nucleus is already the fourth proton emitting Ir isotope. The discovery of the  $^{165}\text{Ir}$ ,  $^{166}\text{Ir}$  and  $^{167}\text{Ir}$  proton emitters was reported in Ref. [20]. In  $^{166}\text{Ir}$  two proton lines were observed and interpreted as the decay of the  $2^-$  ground state and the  $9^+$  isomer corresponding to the  $d_{3/2}$  and  $h_{11/2}$  proton states, respectively, coupled to an  $f_{7/2}$  neutron. The measured proton energies and half lives indicate that the observed proton decaying states in  $^{164}\text{Ir}$  and  $^{170}\text{Au}$  originate from the  $h_{11/2}$  orbital.

The spectroscopic factors deduced from the data can be calculated using the low-seniority shell model [20]. The agreement between the theory and the experiment can be improved significantly by including the coupling to the core  $2^+$  vibrational states [14]. The data on  $^{170}\text{Au}$  and  $^{164}\text{Ir}$  agree quite well with this model.

### 3.5. The isomer studies of the proton emitter daughter $^{140}\text{Dy}$

The deformed proton emitter  $^{141}\text{Ho}$  has two known proton lines corresponding to the ground state [3] and an isomeric state [21]. Excited states in  $^{141}\text{Ho}$  were observed using the Recoil-Decay Tagging method. Based on the properties of the ground-state band a deformation of  $\beta_2 = 0.25$  was deduced for the ground state. A deformation  $\beta_2 = 0.29$  was predicted for  $^{141}\text{Ho}$ . It was suggested that the unexpectedly large signature splitting of the  $7/2^-$  [523] ground-state band could imply triaxiality. In order to learn more about  $^{140}\text{Dy}$  a search for an expected  $K$ -isomer was carried out using an array of Ge detectors placed behind the focal plane of the FMA. A sequence of delayed  $\gamma$ -ray transitions was assigned to  $^{140}\text{Dy}$  and interpreted as the  $8^- \rightarrow 8^+ \rightarrow 6^+ \rightarrow 4^+ \rightarrow 2^+ \rightarrow 0^+$  cascade [22]. Similar results were obtained in an independent experiment at ORNL [23]. From the 203-keV energy of the  $2^+ \rightarrow 0^+$  transition a deformation of  $\beta_2 = 0.25$  was deduced for  $^{140}\text{Dy}$ . This value agrees with the deformation deduced from the ground-state band in  $^{141}\text{Ho}$  [6]. Based on these findings the adiabatic calculations of Ref. [13] suggested a branching ratio of 0.7% for the proton decay to the  $2^+$  state, consistent with an upper limit of 1% found in [6].

#### 4. Upgrades and modifications of the implantation station at ANL

In order to search for proton emitters which are situated even further from the line of stability, and to study the known proton emitters with better accuracy, several modifications of the FMA implantation station were implemented. The first anode of the FMA was replaced by an electrode split in the middle to reduce the amount of scattered beam at the focal plane of the FMA. A new DSSD was installed with 80 horizontal and 80 vertical strips. All strips of the DSSD were equipped with delay-line amplifiers which recover faster after the implantation event. Thanks to these improvements experiments with about 10 times more intense beams are possible and proton decays as fast as  $1 \mu\text{s}$  can be detected.

Because of the long flight path involved, recoil mass separators are not suitable for studies of proton emitters with half lives much lower than  $1 \mu\text{s}$ . In order to circumvent this difficulty an implantation station situated immediately after the target was built. Reaction products, after leaving the target, are slowed down in a Au degrader foil and implanted at the surface of a thin plastic catcher. Their subsequent proton decays are detected in three Si telescopes surrounding the catcher in close geometry. The spectrum of protons corresponding to the known fast  $^{113}\text{Cs}$  ground-state proton decay measured with this setup is shown in Fig. 4.

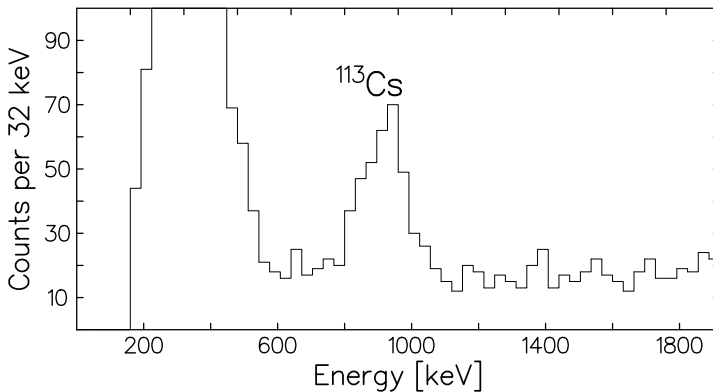


Fig. 4. The proton spectrum collected using a catcher placed downstream from the target. The target was irradiated for about  $20 \mu\text{s}$  and the activity was measured for about  $40 \mu\text{s}$ . The peak at about 900 keV corresponds to the known proton emitter  $^{113}\text{Cs}$ .

## 5. Outlook

Using the improved FMA implantation station one can search for remaining deformed proton emitters in the rare earth region, proton emitters below the  $Z = 50$  line and above the  $Z = 82$  line, more cases of proton-decay fine structure, and excited states in the known proton emitters. Data with better statistics on some of the known proton emitters would also be beneficial.

To allow more detailed comparison between the growing body of experimental information and the theoretical models a better understanding of the Coriolis interaction, non-axial degrees of freedom is required. In odd-odd nuclei the residual interaction between protons and neutrons has to be taken into account.

## REFERENCES

- [1] K.P. Jackson *et al.*, *Phys. Lett.* **B33**, 281 (1970).
- [2] S. Hofmann *et al.*, Proc. 4th International Conf. Nuclei Far from Stability, 1981, eds P.G. Hansen, O.B. Nielsen, CERN Rep. 81-09, p.190.
- [3] C.N. Davids *et al.*, *Phys. Rev. Lett.* **80**, 1849 (1998).
- [4] A.A. Sonzogni *et al.*, *Phys. Rev. Lett.* **83**, 1116 (1999).
- [5] E.S. Paul *et al.*, *Phys. Rev.* **C51**, 78 (1995).
- [6] D. Seweryniak *et al.*, *Phys. Rev. Lett.* **86**, 1458 (2000).
- [7] D. Rudolph *et al.*, *Phys. Rev. Lett.* **89**, 022501 (2002).
- [8] J. Giovinazzo *et al.*, *Phys. Rev. Lett.* **89**, 102501 (2002).
- [9] M. Pfützner *et al.*, *Eur. Phys. J.* **A14**, 279 (2002).
- [10] S. Åberg, P.B. Semmes, W. Nazarewicz, *Phys. Rev.* **C56**, 3011 (1997).
- [11] A.T. Kruppa, B. Barmore, W. Nazarewicz, T. Vertse, *Phys. Rev. Lett.* **84**, 4549 (2000).
- [12] E. Maglione, L.S. Ferreira, R.J. Liotta, *Phys. Rev.* **C59**, 589R (1999).
- [13] H. Esbensen, C.N. Davids, *Phys. Rev.* **C63**, 014315R (2001).
- [14] C.N. Davids, H. Esbensen, *Phys. Rev.* **C64**, 034317R (2001).
- [15] L.S. Ferreira, E. Maglione, *Phys. Rev. Lett.* **84**, 4549 (2000).
- [16] P. Möller, J.R. Nix, W.D. Myers, W.J. Świątecki, *At. Data Nucl. Data Tables* **59**, 185 (1995).
- [17] F. Soramel *et al.*, *Phys. Rev.* **C63**, 031304R (2001).
- [18] H. Mahmud *et al.*, *Phys. Rev.* **C64**, 031303R (2001).
- [19] H. Mahmud *et al.*, Proc. Internat. Conf. on Exotic Nuclei and Atomic Masses, July 2001.
- [20] C.N. Davids *et al.*, *Phys. Rev.* **C55**, 2255 (1997).

- [21] K. Rykaczewski *et al.*, *Phys. Rev. Lett.* **89**, 022501 (2002).
- [22] M. Cullen *et al.*, *Phys. Lett.* **B529**, 42 (2002).
- [23] W. Królas *et al.* *Phys. Lett.* **C65**, 051303 (2002).